

# Analyzing the Optical Properties and Peak Behavior Due to Plasmon Resonance of Silver Cubic-Shape Nanostructures by Means of Discrete Dipole Approximation

Saeed Ranjbar\* and Abbas Azarian

Physics Department, Qom University, Qom, Iran

\*Corresponding author email: Xehi50@yahoo.com

Regular paper: Received: Jan. 11, 2021, Revised: Mar. 21, 2021, Accepted: May. 20, 2021,  
Available Online: Dec. 22, 2021, DOI: 10.52547/ijop.15.2.133

**ABSTRACT**— In this article, the optical properties of silver cubic-shape nanostructures (SCNs) were analyzed by employing the discrete dipole approximation (DDA) in aqueous media. The absorption, dispersion and extinction cross-sections of these nanostructures were calculated based on the wavelength change of the incident light in the visible and near infrared region. Moreover, the height change, wavelength and full width at half maximum (FWHM) of extinction cross-section peaks (from plasmon resonances) based on the size of nanoparticles and the environment dielectric constant were surveyed. The results showed that only two peak modes, named dipole peak and quadrupole peak, exist in this spectrum, such as spherical particles.

**KEYWORDS:** Silver cubic-shape nanostructures, Discrete dipole approximation, Plasmon, Absorption, Dispersion and extinction cross-sections.

## I. INTRODUCTION

In nanostructures, the ratio of boundary atoms to total atoms is relatively high. The behavior of boundary atoms is different from mass atoms. Accordingly, the behavior of nanostructures is different from the mass of a material. Nowadays, nanostructures have received a lot of attention in various fields such as medical sciences [1], biology [2], electronics [3], photonics [4] and chemistry [5] due to their unique optical, electronic, magnetic and quantum properties. From a historical

viewpoint, the dispersion and absorption of electromagnetic waves by nanostructures have resulted in introduction of theories such as Rayleigh, Mai, Ganz, and etc. Theories such as Mai and Ganz are suitable for description of the optical properties of specific geometric shapes. Therefore, other theories such as discrete dipole approximation has been introduced to illustrate the optical properties of a wide range of other nanostructure geometries [6]. By using this theory, the optical properties of nanostructures including adsorption, dispersion and extinction cross-sections, Muller dispersion matrix and pointing vector can be calculated. The optical properties of these particles can be used in the manufacture of optical devices according to considering their behaviors and intensifications.

## II. THEORY OF DISCRETE DIPOLE APPROXIMATION

Discrete dipole approximation called paired dipole approximation is a general method for computing dispersion and absorption of electromagnetic waves by arbitrary geometry particles, which is one of its advantages, that has an acceptable approximation [7]. Discrete dipole approximation allows a great deal of freedom in studying particle shapes. This theory was proposed by Howard Devoe in 1964 and then developed by Edward Purcell and Carlton Pennypacker to calculate the

absorption, scattering and extinction cross-sections of interstellar particles [8], [9].

The particle becomes polarized under radiation of electromagnetic waves. According to this theory, a set of polarizable points (dipoles) are substituted for the target particles. The dipoles interact with each other as well as radiation field. The polarization of dipoles is obtained by solving a linear equation system, which is calculated by its algorithm [9]. Other parameters for dispersion can be calculated using the polarizations obtained [10].

As mentioned earlier, the radiation of electromagnetic waves induces polarization of intended particles, given by the equations:

$$P(r_i) = \alpha_i \cdot E_{loc}(r_i) \quad (1)$$

where  $\alpha_i$  is polarization in point  $i$  and  $E_{loc}(r_i)$  is the sum of radiation field. The induction field is given by the equation [11]:

$$E_{loc}(r_i) = E_{inc}(r_i) + E_{ind}(r_i) \quad (2)$$

Induction field  $E_{loc}(r_i)$  is the result of induction field of N-1 of another dipole that is defined as  $-\sum_{j \neq i} A_{ij} P_j$ , therefore if the radiation wave is flat, we will have:

$$E_{loc}(r_i) = E_0 \exp(ik \cdot r_i) - \sum_{j \neq i} A_{ij} \cdot P_j \quad (3)$$

$E_0$  is radiation wave amplitude and  $A_{ij}$  is a matrix that is defined below:

$$A_{ij} = \frac{\exp(ikr_{ij})}{r_{ij}} \left[ k^2 (\hat{r}_{ij} \hat{r}_{ij} - I_3) + \frac{ikr_{ij}}{r_{ij}^2} (3\hat{r}_{ij} \hat{r}_{ij} - I_3) \right] \quad (4)$$

Here,  $k = \frac{\omega}{c}$ ,  $r_{ij} = |r_i - r_j|$  and polarization is as below:

$$\alpha_i = \frac{\alpha^{CM}}{1 + \alpha^{CM} \left[ \left( b_1^{LDR} + \varepsilon b_2^{LDR} + \varepsilon s b_3^{LDR} \right) \left( \frac{k^2}{d} - \frac{2}{3} ik^3 \right) \right]} \quad (5)$$

In the above equation,  $\varepsilon$  is dielectric function,  $\alpha^{CM}$  is Clausius-Mossotti Polarizability and other constants are as below:

$$s = \sum_j \left( \hat{a}_j \cdot \hat{e}_j \right) \quad (6)$$

$$\alpha^{CM} = \frac{3d^3}{4\pi} \frac{\varepsilon - 1}{\varepsilon + 2} \quad (7)$$

$$b_1^{LDR} \approx 1.8915316, \quad b_2^{LDR} \approx -0.1648469, \\ b_3^{LDR} \approx 0.7700004$$

It is worth mentioning that  $\hat{a}_j$  is the vector in direction of radiation and  $\hat{e}_j$  shows polarization direction. The polarization is achieved based on equation below [12]:

$$P(r_i) = \alpha_i \cdot \left( E_0 \exp(ik \cdot r_i) - \sum_{j \neq i} A_{ij} \cdot P_j \right) \quad (8)$$

Now by using the calculated polarization, the absorption, dispersion and extinction cross-sections can be calculated [12]:

$$C_{abs} = \frac{4\pi k}{|E_0|^2} \sum_{j=1}^N \left\{ \text{Im} \left[ P_j \cdot (\alpha_j^{-1})^* P_j^* \right] - \frac{2}{3} k^3 |P_j|^2 \right\} \quad (9)$$

$$C_{ext} = \frac{4\pi k}{|E_0|^2} \sum_{j=1}^N \left\{ \text{Im} \left( E_{inc,j}^* \cdot P_j \right) \right\} \quad (10)$$

The cross-sections are as follows:

$$C_{sca} = C_{ext} - C_{abs} \quad (11)$$

where  $C_{abs}$ ,  $C_{ext}$  and  $C_{sca}$  are absorption, extinction, and dispersion cross-sections, respectively.

### III. RESULTS

The nature of the material used in nanomaterial production affects optical, mechanical, magnetic and other properties of nanostructures. More than half of the materials in the environment are metals. Silver is unique due to the presence of plasmon resonance bond in visible region. In this article, absorption, dispersion and extinction cross-sections of silver cubic-shape nanostructures will be discussed by employing discrete dipole approximation. Some factors affecting the above mentioned attributes will be discussed, as well. Type of material used, shape and environment are among the factors affecting specific properties of silver cubic-shape nanostructures. Cubic shape consist of many vertices and edges, so higher plasmon modes than dipole will be created. Therefore, many peaks are predicted in absorption, dispersion and extinction cross-sections, especially in higher heights [13].

It is worth mentioning that the analyses here are for a situation that the incident wave radiates perpendicular to the dimension of silver cubic-shape nanoparticle and direction of landing on any side is similar because of the symmetry of the square cube.

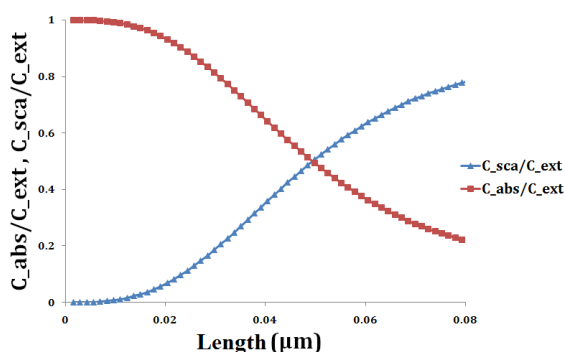


Fig. 1. The ratio of the scattering and absorption cross-sections to the extinction cross-section (cross-section factors) in terms of the length of silver cubic shape nanoparticles for a wavelength of 0.560  $\mu\text{m}$ .

Figure 1 illustrates the ratio of absorption and dispersion cross-sections to extinction cross-section (absorption and dispersion factors) for silver cubic-shape nanoparticles based on their length. The wavelength of optional incident light is 0.560  $\mu\text{m}$ . Clearly, for smaller particles, the dominant process is absorption while the

dispersion share is almost zero. By increasing the size of the particle, gradually the absorption share decreases and dispersion process prevails. For particles larger than 0.05  $\mu\text{m}$  in size, the dispersion share is more than absorption phenomenon. This behavior can be seen for the cross-section of silver spherical nanostructures according to Mai theory [14].

Figure 2 shows the cross-sections of absorption, scattering and extinction for silver nanoparticles with a length of 0.02  $\mu\text{m}$  as a function of the wavelength of the incident light. As it can be seen, absorption is the prevailing phenomenon and scattering has a small share, most probably due to the small length of particle. Several peaks were observed in the mentioned cross-sections. The peaks at 430 and 0.47  $\mu\text{m}$  can be attributed to dipole and quadrupole modes, respectively.

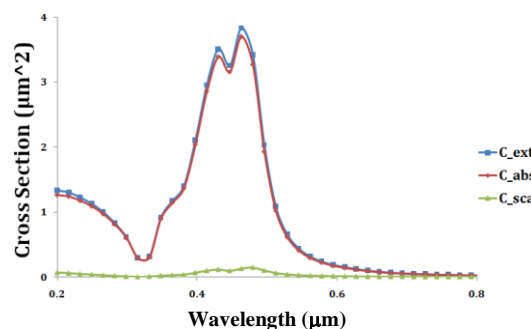


Fig. 2. Variations of the absorption, dispersion and extinction cross-sections of particles with a length of 0.02  $\mu\text{m}$  as in terms of the wavelength of the incident light.

The peak height, FWHM and wavelength of each plasmon mode were evaluated. Figure 3 shows the variations of a) peak height, b) peak wavelength and c) FWHM of plasmon resonance peaks of dipole and quadrupole modes in the extinction cross-section at 0.56  $\mu\text{m}$ . As it is shown in Fig. 3(a), by increasing nanoparticle length, the peak height of the plasmon resonance of dipole and quadrupole modes increased. The peak height of the plasmon resonance for dipole and quadrupole reached its maximum at 0.04  $\mu\text{m}$  and at 0.06  $\mu\text{m}$ , respectively. The plasmon resonance height decreased for larger particles due to the emergence of higher modes than quadrupole, the height of peaks for the mentioned two modes declined. According to Fig. 3(b), for the

dipole mode by increasing nanoparticle length, the wavelengths of plasmon resonance peaks were almost constant. However, the wavelengths of plasmon resonance peaks increased for the quadrupole mode as nanoparticle length increased. According to Fig. 3(c), a slow increase in FWHM of the peaks in lengths less than  $0.05 \mu\text{m}$  were observed for both dipole and quadrupole modes. FWHM of the peaks significantly increased for lengths more than  $0.06 \mu\text{m}$ . The media used for nanoparticles was water ( $\epsilon_{med}=1.33$ ) for all samples in Fig. 3.

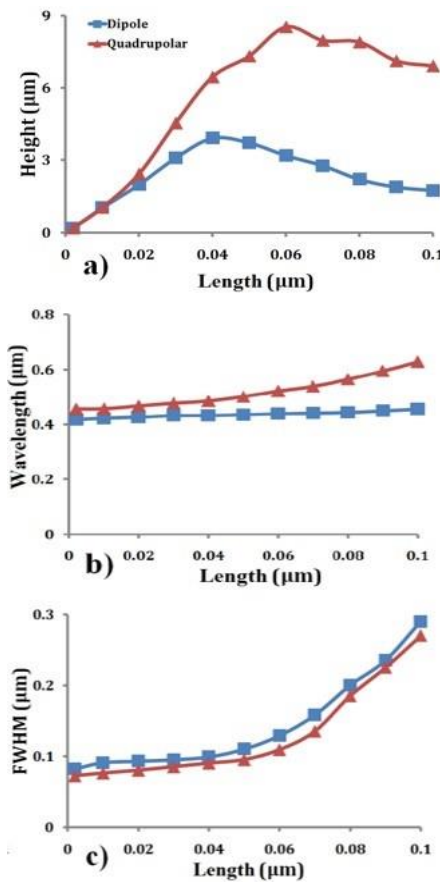


Fig. 3. The variations of a) peak height, b) peak wavelength and c) FWHM of plasmon resonance peaks of dipole and quadrupole modes in the extinction cross-section in terms of the length of silver cubic shape nanoparticles at  $0.56 \mu\text{m}$ .

As it was mentioned previously, height and location of peaks varies by any change in dielectric constant of the environment. For example, if the size of nanoparticles is very small (Rayleigh approximation is dominant), resonances happen when [15]:

$$\epsilon'_{par} = -2\epsilon_{med} \quad (12)$$

where  $\epsilon_{med}$  is the dielectric constant of the environment and  $\epsilon'_{par}$  is the real part of the dielectric constant of nanoparticle. As the dielectric constant of the environment increases, resonance occurs for larger amounts of real part of the dielectric function of the nanoparticle. In most of metals including silver, increasing length leads to higher negative values in the real part of the dielectric function. So, it is expected that the wavelength of plasmon resonance peak moves to longer wavelengths by increasing the dielectric constant of the environment according to Rayleigh approximation [14].

Figure 4 shows the variations of extinction cross-section as a function of incident wavelength for silver cubic-shape nanoparticles with the length of  $0.02 \mu\text{m}$  in different environments. In all cases, two peaks were observed in analyzed region. As the dielectric constant of environment increased, the locations of plasmon peaks shifted toward the longer wavelengths (red shift) [14].

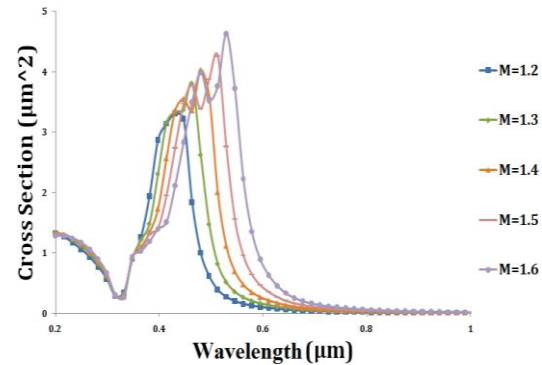


Fig. 4. Extinction cross-section as a function of the wavelength of incident light for different environments for silver cubic nanoparticles with a length of  $0.02 \mu\text{m}$ .

Herein, we will discuss the impact of dielectric constant of the environment on absorption and dispersion factors, height, wavelength and FWHM of plasmon resonance peaks.

Figure 5 shows the absorption and dispersion factors of silver cubic shape nanoparticles with length of  $0.02 \mu\text{m}$ , as the dielectric constant of the environment changes. Any variation in environmental dielectric constant influence the dominant process. The dominant process in the analyzed region for small silver cubic-shape

nanoparticles ( $0.02\ \mu\text{m}$  length) was absorption. However, as the dielectric constant of environment increased, absorption factor decreased and dispersion factor increased.

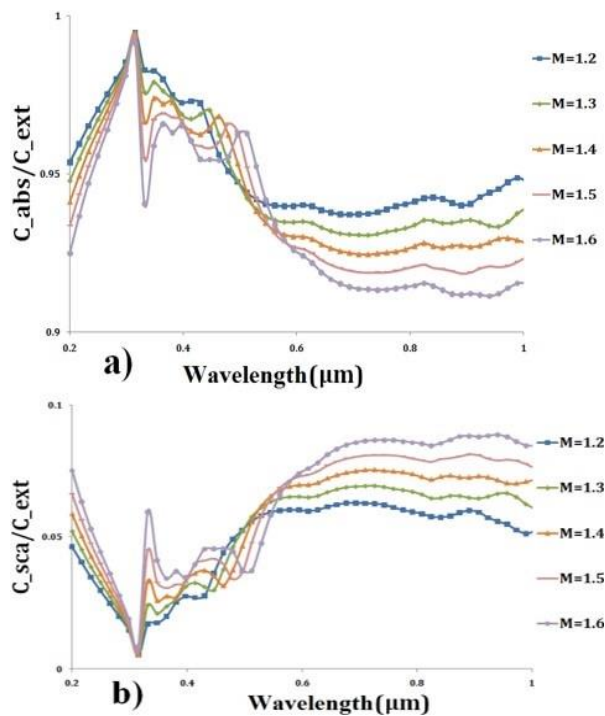


Fig. 5. The variations of dispersion and absorption factors as a function of the wavelength of incident light in different environments for silver cubic nanoparticles with a length of  $0.02\ \mu\text{m}$ .

Figure 6 shows the impact of the refractive index of the environment on a) height b) wavelength c) FWHM of peaks for the extinction cross-section of particle length of  $0.02\ \mu\text{m}$ .

The height of the plasmon resonance peak of dipole and quadrupole modes increased by increasing the refractive index of the environment. Furthermore, the wavelength and FWHM of these peaks increased as the refractive index of the environment increased. In addition, the wavelength of plasmon resonance peak showed linear behavior with increasing refractive index of the environment. According to previous studies, the linear behavior has also been observed for silver spherical nanoparticles [16], [17].

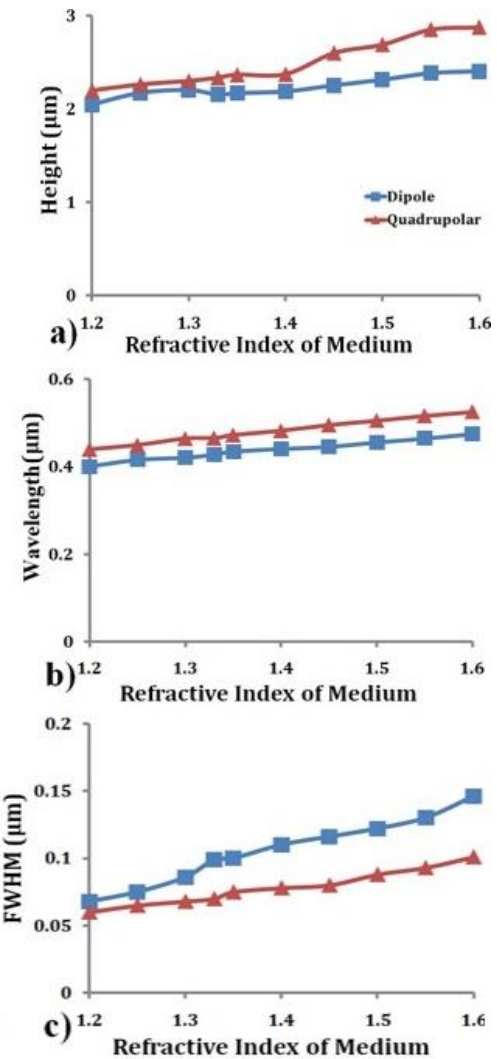


Fig. 6. Impact of environmental refractive index on a) height, b) wavelength and c) FWHM of peaks in the extinction cross-section for silver cubic nanoparticles with a length of  $0.02\ \mu\text{m}$ .

#### IV. CONCLUSION

In this paper, the adsorption, dispersion and extinction cross-sections for silver cubic nanostructures were investigated using a discrete dipole approximation. The peaks at cross-section results from the particulate plasmon resonance. These resonances occur due to the coupling of the applied electric field with particle plasmons at certain wavelengths. In the visible region, only low-order plasmon modes (dipole and quadrupole modes) appear due to the small size of the nanostructures compared to the incident wavelength. This can be attributed to the multipolar distribution of conduction electrons on the surface of nanoparticles [18], [19].

According to the results, the dominant process for very small nanoparticles was adsorption phenomenon while the scattering share was almost zero. However, as the particle size increased, the adsorption gradually decreased and the dispersion process became dominant. In addition, when the length of silver nanoparticles increased, the heights of plasmon resonance peaks of dipole and quadrupole modes showed an ascending trend. In larger lengths due to the emergence of higher modes than quadrupole, the height of peaks for the mentioned two modes declined. Increase in environmental refractive index led to increase in height, wavelength and FWHM of the mentioned peaks.

## REFERENCES

- [1] O.V. Salata, "Applications of nanoparticles in biology and medicine," J. Nanobiotechnol. Vol. 2, no. 1, pp. 1-6, 2004.
- [2] C.J. Murphy, A.M. Gole, J.W. Stone, P.N. Sisco, A.M. Alkilany, E.C. Goldsmith, and S.C. Baxter, "Gold nanoparticles in biology: beyond toxicity to cellular imaging," Accounts Chem. Res. Vol. 41, no. 12, pp. 1721–1730, 2008.
- [3] M. Homberger and U. Simon, "On the application potential of gold nanoparticles in nanoelectronics and biomedicine," Philos. Trans. R. Soc. Math. Phys. Eng. Sci. Vol. 368, no. 1915, pp. 1405–1453, 2010.
- [4] J. Conde, J. Rosa, J.C. Lima, and P.V. Baptista, "Nanophotonics for molecular diagnostics and therapy applications," Int. J. Photoenergy, Vol. 2012, 2012.
- [5] M.C. Daniel and D. Astruc, "Gold nanoparticles: assembly, supramolecular chemistry, quantum-size-related properties, and applications toward biology, catalysis, and nanotechnology," Chem. Rev. vol. 104, no. 1, pp. 293–346, 2004.
- [6] M.A. Yurkin and A.G. Hoekstra, "The discrete dipole approximation: an overview and recent developments," J. Quantum Spectrosc. Radiat. Transf. Vol. 106, no. 1, pp. 558–589, 2007.
- [7] M.A. Yurkin and A.G. Hoekstra, "The discrete-dipole-approximation code ADDA: capabilities and known limitations," J. Quantum Spectrosc. Radiat. Transf. Vol. 112, no. 13, pp. 2234–2247, 2011.
- [8] P.J. Flatau and B.T. Draine, "Discrete-dipole approximation for scattering calculations," J. Opt. Soc. Am. A, Vol. 11, pp. 1491–1499, 1994.
- [9] B.T. Draine and P.J. Flatau, User Guide for the discrete dipole approximation code DDSCAT 7.3. <<http://www.arxiv.org/abs/1202.3424>>, 2012.
- [10] V.L. Loke, M.P. Mengüç, and T.A. Nieminen, "Discrete-dipole approximation with surface interaction: Computational toolbox for MATLAB," J. Quantum Spectrosc. Radiat. Transf. Vol. 112, no. 11, pp. 1711–1725, 2011.
- [11] R. Schmehl, B.M. Nebeker, and E.D. Hirleman, "Discrete-dipole approximation for scattering by features on surfaces by means of a two-dimensional fast Fourier transform technique," J. Opt. Soc. Am. A, Vol. 14, no. 11, pp. 3026–3036, 1997.
- [12] I. Ayrancı, R. Vaillon, and N. Selcuk, "Performance of discrete dipole approximation for prediction of amplitude and phase of electromagnetic scattering by particles," J. Quantum Spectrosc. Radiat. Transf. Vol. 103, no. 1, pp. 83–101, 2007.
- [13] A.L. González and C. Noguez, "Influence of morphology on the optical properties of metal nanoparticles," J. Comput. Theor. Nanosci. Vol. 4, no. 2, pp. 231–238, 2007.
- [14] C.F. Bohren and D.R. Huffman, *Absorption and scattering by small particles*, John Wiley, pp. 82–129, 1998.
- [15] M. Quinten, *Optical properties of nanoparticle systems: Mie and beyond*. John Wiley & Sons, 2010.
- [16] A. Moroz, "Depolarization field of spheroidal particles," J. Opt. Soc. Am. B, Vol. 26, no. 3, pp. 517–527, 2009.
- [17] A. Wokaun, J.P. Gordon, and P.F. Liao, "Radiation damping in surface-enhanced Raman scattering," Phys. Rev. Lett. Vol. 48, no. 14, pp. 957–960, 1982.
- [18] M.P. Marder, *Condensed matter physics*. John Wiley & Sons, 2010.
- [19] C. Sönnichsen, T. Franzl, T. Wilk, G. Von Plessen, and J. Feldmann, "Plasmon resonances in large noble-metal clusters," New J. Phys. Vol. 4, no. 1, pp. 93 (1-8), 2002.



**Saeed Ranjbar** was born on Sept. 7, 1987 in Tehran, Iran. He received his MSc in Atomic and Molecular Physics from Qom University, Qom, Iran in 2014.



**Abbas Azarian** was born on June 5, 1979 in Tehran, Iran. He received his PhD in Condensed Matter Physics from Sharif University of Technology, Tehran, Iran in 2008. He is an associate professor in Physics Department of Qom University. He was known as a top researcher in 2014.

**THIS PAGE IS INTENTIONALLY LEFT BLANK.**